FEBS Letters 545 (2003) 86–95 FEBS 27219

Minireview

Flagellar movement driven by proton translocation

David F. Blair

Department of Biology, University of Utah, 257 South 1400 East, Salt Lake City, UT 84112-0840, USA

Received 10 February 2003; accepted 12 February 2003

First published online 22 April 2003

Edited by Bernard L. Trumpower

Abstract The bacterial flagellar motor couples ion flow to rotary motion at high speed and with apparently fixed stoichiometry. The functional properties of the motor are quite well understood, but its molecular mechanism remains unknown. Recent studies of motor physiology, coupled with mutational and biochemical studies of the components, put significant constraints on the mechanism. Rotation is probably driven by conformational changes in membrane–protein complexes that form the stator. These conformational changes occur as protons move on and off a critical Asp residue in the stator protein MotB, and the resulting forces are applied to the rotor protein FliG.

Key words: Bacterial motility; Molecular motor; Ion channel

1. Introduction

Bacterial flagella are helical propellers turned by rotary motors in the cell membrane [1]. The fuel for rotation is the membrane gradient of ions, H^+ in most neutrophiles [2–4] and Na^+ in alkalophiles and marine *Vibrio* species [5]. Bacteria control their flagella so that swimming is directed toward environments that promote survival. In most species, the motors can rotate either clockwise (CW) or counterclockwise (CCW), and cells direct their movement by regulating switching between the two directions [6,7]. In *Escherichia coli* or *Salmonella*, for example, CCW rotation allows the several filaments on a cell to join in a bundle and drive the cell smoothly forward (a 'run'), whereas CW rotation disrupts the filament bundle and causes rapid somersaulting (a 'tumble'). When a cell swims in an isotropic environment, the flagellar motors reverse direction at random intervals, and the trajectory is a random walk consisting of runs of about 1 s alternating with short tumbles [8]. In a spatial gradient of a chemical attractant such as serine or maltose, cells increase the duration of runs that happen to be carrying them up the gradient, while not altering (or only slightly shortening) runs down the gradient, thus biasing their movement toward regions of higher attractant concentration [9].

Much is known about the performance of the flagellar rotary motor and how it varies with load, membrane gradient, and other external variables. Ultrastructural studies have provided an impressive picture of the overall shape of the flagellar motor, and genetic and biochemical studies have identified the proteins that function in assembly and rotation of the flagella. The molecular mechanism of rotation remains poorly understood, however, mainly due to a lack of high-resolution structural information. This minireview will summarize recent insights into the mechanism obtained from physiological and mutational studies, and initial efforts at structure determination. Other reviews provide a fuller discussion of the important topics of flagellar assembly [10–12], direction switching [13,14], and theories of the rotation mechanism [15–17].

2. Overview of flagellar structure

Most of the mass of the flagellum is in the long helical filament (Fig. 1A). The filament is formed from thousands of copies of a single protein (or a few closely related proteins) called flagellin, arranged on a helical lattice to form a hollow tube. A crystal structure was recently solved for most of the flagellin protein, revealing the molecular basis of subunit packing in the filament and the variations in packing that give rise to its helical shape [18]. The base of the filament is joined to a slightly thicker, flexible structure termed the hook, joined in turn to a set of rings mounted on a rod [19–21]. The exterior parts of the flagellum serve mechanical roles: The rigid filaments convert rotary motion into thrust, while the hook confers flexibility to allow the different flagella on a cell to join into a synchronously rotating bundle during smooth swimming. The torque for flagellar rotation is generated at the base, in parts of the structure in and near the cytoplasmic membrane.

Single-particle reconstructions of the flagellar basal body have achieved a resolution approaching 20 Å, revealing much detail in the shapes of the rings and rod (Fig. 1B) [21,22]. The rings are named for their locations relative to cell-envelope structures. The LP-ring assembly is at the level of the outer (lipopolysaccharide) membrane and peptidoglycan layer, and is thought to function as a bushing for the central rod. The MS-ring is within and above the cytoplasmic membrane (M = membrane; S = supramembrane). The MS-ring and the cell-proximal part of the rod are formed from a single protein, FliF [23]. Mounted on the cytoplasmic face of the MS-ring is a drum-shaped structure termed the C-ring [20,21]. Good en face views of the C-ring show fine structure with either 33- or 34-fold rotational symmetry, depending on the specimen (Fig. 1C) [24].

The structure seen in the single-particle reconstructions is

E-mail address: blair@bioscience.utah.edu (D.F. Blair).

Abbreviations: CW, clockwise; CCW, counterclockwise

0014-5793/03/$22.00
doi:10.1016/S0014-5793(03)00397-1

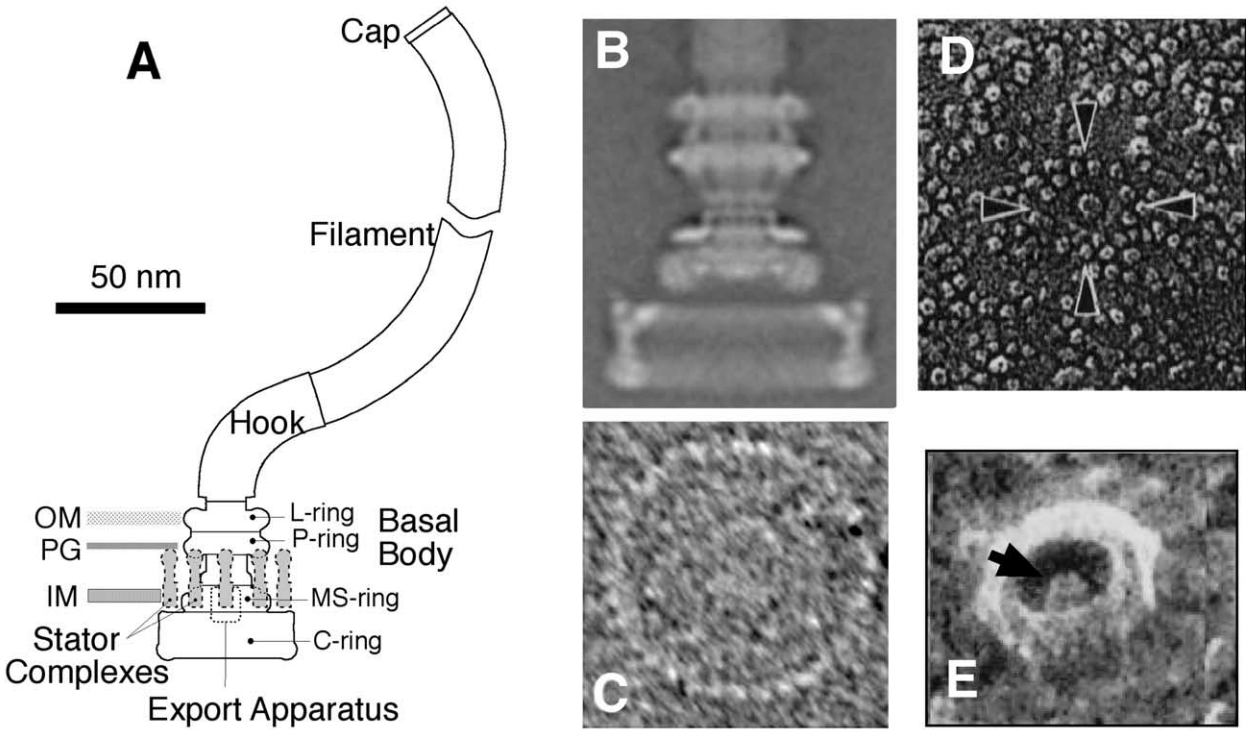

Fig. 1. A: Diagram of the flagellum in a Gram-negative bacterium. Gram-positive species lack the LP-ring assembly. Only a fraction of the full filament length is shown, as it is quite long on this scale (ca. 10 μm). OM, outer membrane; PG, peptidoglycan; IM, inner membrane. B: Electron micrographic reconstruction of the flagellar basal body – side view. The image was obtained by averaging micrographs of single particles embedded in vitreous ice. The cytoplasm is down and the hook is up; only the bottom-most portion of the hook is visible. C: En face view of the C-ring, viewed from the cytoplasmic side. Subunit structure is clearly visible. Rotational averaging and Fourier transforms demonstrate a 34-fold rotational symmetry for this specimen [24] (panels B and C from D.J. DeRosier, with permission). D: Circular array of membrane-embedded particles, thought to be MotA/MotB protein complexes, that is the stator. The larger particle in the center is the cell-proximal part of the basal-body rod. The inner diameter of this particle ring is about 30 nm. The image is from *Salmonella* but similar structures have been seen in several species (from S. Khan, with permission). E: Central protrusion within the C-ring that is probably the export apparatus essential for assembly of exterior structures of the flagellum. The view is from inside the cell (from S.-I. Aizawa, with permission).

one that has survived purification, and is known to lack some important components. The basal structure in Fig. 1B,C is probably just the rotating part (the rotor) of the motor. The non-rotating part (the stator) is a circular array of protein complexes in the membrane around the rotor, which have been seen in freeze-fracture images (Fig. 1D) [25]. The number of particles in each circular array ranges from 10 to 16, varying between species and also from motor to motor. The inner diameter of the array varies from 20 to 30 nm, depending on the species [25] and the method of sample preparation [26]. As discussed further below, the individual stator complexes appear equivalent and can function independently to produce torque [27,28].

During flagellar assembly, flagellin and certain other components reach their destinations in the structure by being exported through a central channel [10,12]. Export is carried out by an apparatus related to the type-III secretion systems utilized by pathogens (or symbiotic species) to pump effector proteins into their hosts [29,30]. Deep-etch replica images of the inner surfaces of cells show a protrusion near the center of the C-ring that is probably this export apparatus, or a part of it (Fig. 1E) [31,32].

3. Proteins that function in rotation

A bacterial flagellum contains about two dozen proteins. Most of these play structural roles, and can be mapped to particular features in the basal body, hook, or filament [10,12]. Genetic studies suggest that only the proteins MotA, MotB, FliG, FliM, and FliN function specifically in motor rotation. Mutations in only these five proteins can prevent rotation while not preventing flagellar assembly [33]. MotA and MotB are membrane proteins [34,35] that form the stator [25,36], and function together to conduct ions across the membrane [37,38]. FliG, FliM, and FliN form a rotor-mounted assembly termed the switch complex, which is essential for flagellar assembly and CW–CCW switching as well as for rotation [39]. The probable organization of these five motor proteins within the flagellum is illustrated in Fig. 2.

The circular arrays of membrane particles seen in freeze-fracture images (Fig. 1D) are almost certainly the MotA/MotB complexes, because they are not observed in mutants lacking the *motA* or *motB* gene [25]. The precise relationship between the MotA/MotB complexes and the rotor is not clear, however. The inner diameter of the particle rings is about 30 nm [26]. (Certain images show a significantly smaller diameter but this appears to be induced by deep etching [26].) This is similar to the diameter of the MS-ring, and significantly less than that of the C-ring (45 nm; Fig. 1B). Because the particles seen in freeze-fracture images were viewed from the periplasmic side of the membrane, their arrangement likely reflects the periplasmic domains of MotB molecules, which are fairly

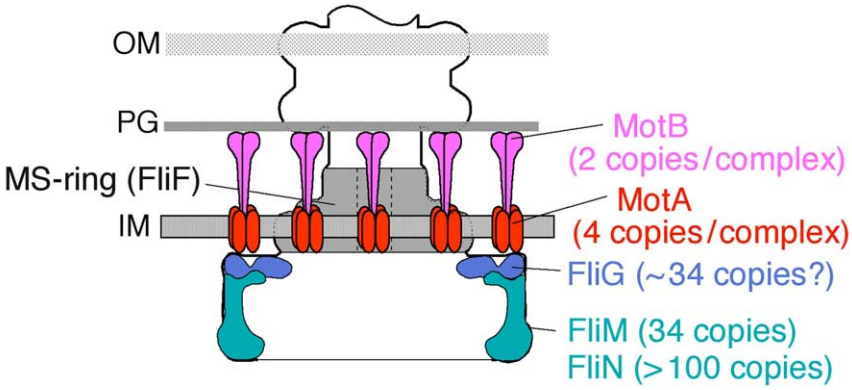

Fig. 2. Proteins that function in rotation. The MotA and MotB proteins form the stator complexes, anchored to the cell wall by a putative peptidoglycan-binding motif in the periplasmic domain of MotB. Each motor contains several (as many as eight) stator complexes, each with composition $MotA_4MotB_2$. FliF does not function directly in rotation, but forms the MS-ring that is the mounting surface for the 'switch complex' comprising FliG, FliM, and FliN. FliG is known to contact the MS-ring directly, whereas FliM and FliN are somewhere farther down in the C-ring. Exact protein locations are not known, and so details of the pictured arrangement are speculative.

large (Fig. 2). Interaction with the rotor occurs through the cytoplasmic domain of MotA, on the other side of the membrane [40]. The rotor–stator interface could thus be at a greater radius, possibly near the outer edge of the C-ring (Fig. 2).

FliM and FliN together form most of the C-ring [21,32]. FliM appears to function mainly in CW–CCW switching [41], and is the target for binding phospho-CheY, the signaling molecule that is the output of the chemotaxis pathway [42]. Mutational studies indicate that FliN has relatively small roles in switching and rotation [43,44]; it might have a mainly structural role, and/or could function in flagellar assembly [45]. FliG is the rotor protein most directly involved in rotation [43,44]. The C-terminal domain of FliG, in particular, functions specifically in rotation [44] and interacts with the stator protein MotA [40]. FliG binds to the protein FliF that forms the MS-ring [46], and difference electron micrographs of basal bodies with or without FliG show that at least part of FliG is present near the bottom of the MS-ring [22]. The precise location of FliG is not known, however.

The switch complex contains many copies of each protein. By quantitative immunoblots and high-performance liquid chromatography, each motor is estimated to contain 34 (± 6) FliM molecules and 111 (± 13) FliN molecules [32]. Given the 34- or 33-fold or symmetry seen in en face views of the C-ring [24], it is likely that the actual number of FliM molecules is close to 34, varying slightly from motor to motor. Equilibrium sedimentation experiments with purified switch-complex proteins of *Thermotoga maritima* gave evidence of a stable FliN tetramer and a stable FliM:FliN complex with 1:4 stoichiometry (P. Brown and D.F. Blair, unpublished). This suggests that each motor might contain 136 (4×34) copies of FliN. The number of FliG molecules is estimated to be around 44 per motor [32], somewhat greater than the number estimated for FliM but probably still consistent with a 1:1 ratio of FliG to FliM, given the uncertainties.

FliG binds to FliM [47–49], and the simplest hypothesis is that they are present in equal numbers in the motor, about 34 copies each. However, some other data suggest that FliG might be present in fewer copies than FliM. When FliG is linked to FliF by a genetic fusion (recall that FliF forms the MS-ring), the basal bodies appear essentially normal and the motors continue to work fairly well [22,50]. The FliF:FliG stoichiometry should then be 1:1, and by the foregoing reasoning the number of FliF subunits would also be 34. Two estimates of FliF stoichiometry were both in the neighborhood of 26. Uncertainties in those estimates might be great enough to allow a value of 34. But if the estimate of 26 FliF subunits is accurate, there must be a mismatch in subunit number somewhere, most likely between FliG and FliM. In an extension of this idea, DeRosier and co-workers propose that the positions of symmetry mismatch on the rotor might form sites of interaction with the stator, and function in the generation of torque [24].

4. Flagellar motor physiology

Soon after the discovery that flagella rotate [1], Silverman and Simon [6] described an experiment in which cells were attached to coverslips by single flagellar filaments and the rotation of individual motors was monitored by the resulting rotation of the cell body. Such 'tethered' cells rotate relatively slowly (ca. 10 Hz), owing to the large viscous load. Berg showed that the rotation is quite smooth and must therefore occur in relatively small steps [51]. Tethered-cell assays proved especially informative when joined to means for controlling the membrane proton gradient. Experiments with tethered, artificially energized cells produced the following key observations [52–54]: (1) For a given protonmotive force (Δp), the rotation speed varies inversely with the viscosity of the medium, implying a constant torque. (2) The torque is proportional to Δp, up to at least 150 mV. (3) For a given Δp, the torque does not vary significantly with temperature between 5°C and 40°C. (4) For a given Δp, the torque is the same in D_2O and H_2O.

The lack of any dependence on solvent isotope or temperature indicates that at the low speeds of tethered cells, the motor is not limited by rates of ion transfer, or any thermally promoted processes (such as conformational changes or movements within the motor components). In this low-speed regime, the speed appears to be determined by the energetics of the overall process, rather than by kinetic factors. The linear relationship between torque and protonmotive force is most simply explained by saying that slow-turning motors can convert chemical energy into mechanical energy with high efficiency, so that the work done in one revolution (2π times the torque) equals the total energy available from the proton

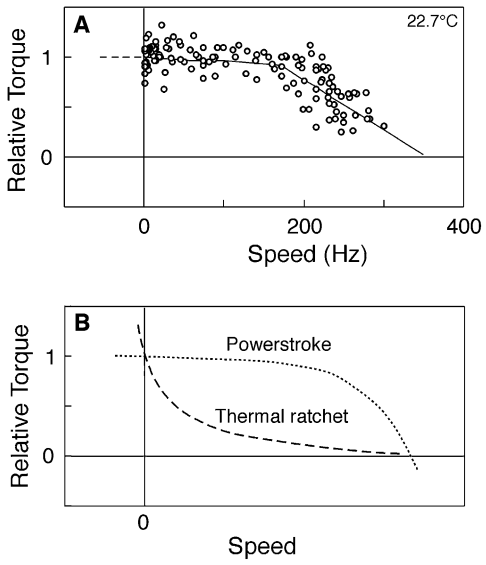

Fig. 3. A: Torque–speed relation of the flagellar motor of *E. coli*, measured by monitoring the rotation of small beads attached to flagellar stubs [56] (from H.C. Berg, with permission). Additional measurements using an optical trap [63] or electrorotation [58] show that the torque–speed relation continues essentially flat into the region of negative speed, as indicated by the dashed line. B: Predicted torque–speed relations for a hypothetical motor that utilizes either a powerstroke mechanism in which chemical energy is used to actively drive motion of the rotor, or a thermal ratchet mechanism in which chemical energy is used to bias movements that are driven thermally. The thermal ratchet mechanism predicts a large drop in torque at even relatively low speeds, which is not observed. For a fuller discussion, see ref. [58].

gradient ($e\Delta p$ times the number of protons used per revolution).

The viscous load is smaller when motors turn flagellar filaments [55] or filament stubs attached to small spheres [56], and load can also be reduced by application of an external torque [15,57,58]. The rotation of such lightly loaded motors can be monitored by various light-microscopic methods [55,56,59]. Such measurements show that when the load is light the flagellar motors of *E. coli* turn at 300 Hz or faster, and the speed depends on both temperature and solvent isotope [55,56]. Thus, when the external load is light the speed of the motor is determined by rates of internal processes, including (but not necessarily restricted to) rates of proton dissociation. Observations on Na^+-driven motors of *Vibrio* provide additional evidence that ion movements are rate limiting when the external load is light. Na^+-driven motors have been clocked at 1700 Hz, five times faster than the highest speeds recorded for H^+-driven motors [59]. Lithium can substitute for sodium in the *Vibrio* motor; the motor speed in Li^+ is about the same as in Na^+ when the viscous load is heavy but about four-fold slower when the load is light [60].

Although the top speed of the motor is evidently limited by one or more proton-dissociation processes, the speed of the *E. coli* motor does not vary appreciably with external pH in the range of 4.7–8.8, even when the load is light [61]. This insensitivity to pH is notable, as the relative contributions of $\Delta\Psi$ and ΔpH to Δp should vary greatly across this pH range [62]. The *E. coli* motor evidently has features that ensure that the pH gradient and electric-potential gradient are not only equivalent thermodynamically but are nearly equivalent kinetically. The situation may be different in the motors of *Bacillus subtilis* and *Streptococcus* (both Gram-positive organisms) which show a greater dependence on pH [3,54].

The torque vs. speed characteristic of the motor is of particular interest for understanding the mechanism. Measurements employing electrorotation to control the load showed that the motor torque is approximately constant for speeds up to a particular 'knee' value, thereafter decreasing approximately linearly to zero [15]. The main features of this torque–speed relationship were subsequently confirmed in experiments that used small beads on flagellar stubs to control the load. (Fig. 3A) [56]. An apparent barrier to backward rotation seen in the electrorotation experiments was later shown to be due to ellipticity in the rotating electric field used [58,63]. This influenced only the measurements on cells forced to rotate backwards (i.e. in a direction opposite to the motor torque), and did not alter the shape of the torque–speed relationship measured at positive rotation speeds. As discussed by Berry and Berg [58], a torque–speed relationship with this shape is indicative of a 'powerstroke' mechanism in which chemical energy is used directly to drive rotation, and argues persuasively against a 'thermal ratchet' mechanism in which chemical energy is used to rectify thermally driven movements of motor components (Fig. 3B).

The peripheral location of the MotA/MotB stator complexes suggests that these proteins could be incorporated last into otherwise complete motors. 'Resurrection' experiments of Berg and co-workers show that this is indeed the case [27,28]. When *motA* or *motB* mutant cells were tethered and wild-type MotA or MotB proteins subsequently expressed from an inducible plasmid, the initially paralyzed cells began to rotate, slowly at first and then accelerating to normal speed in a series of equal steps. As many as eight steps were seen, showing that MotA and MotB are components in several, possibly eight, independent torque-generating units [28]. Sodium-driven motors likewise contain several independent torque generators, as judged by stepwise decreases in torque observed in motors undergoing inhibition by a sodium-channel blocker. In that case, the number of torque generators was estimated to be between five and nine [64].

More recently, resurrection experiments have been carried out on motors driving a light load (small beads) [65]. In contrast to tethered cells, which showed equal steps in speed, when the load was light the first torque generator installed in a motor drove rotation at a large fraction of the full final speed. This implies that the torque generators have a high duty ratio, i.e. they constrain the movement of the rotor most of the time. If a stator complex were disengaged from the rotor for an appreciable time, then additional torque generators in the motor should increase its speed, even under light load.

As noted, a number of observations on tethered cells suggest that the motor has a fixed proton stoichiometry and is capable of converting chemical energy into work with high efficiency provided the speed is low. The measured motor torque can be used to estimate the proton stoichiometry under this assumption of tight coupling, and in any case places a lower bound on the stoichiometry, on thermodynamic grounds. Measurements of motor torque vary somewhat, but a recent measurement that appears reliable is $\sim$290 pN nm per torque generator, or $\sim$2300 pN nm for a motor with a full complement of eight torque generators [65]. Assuming

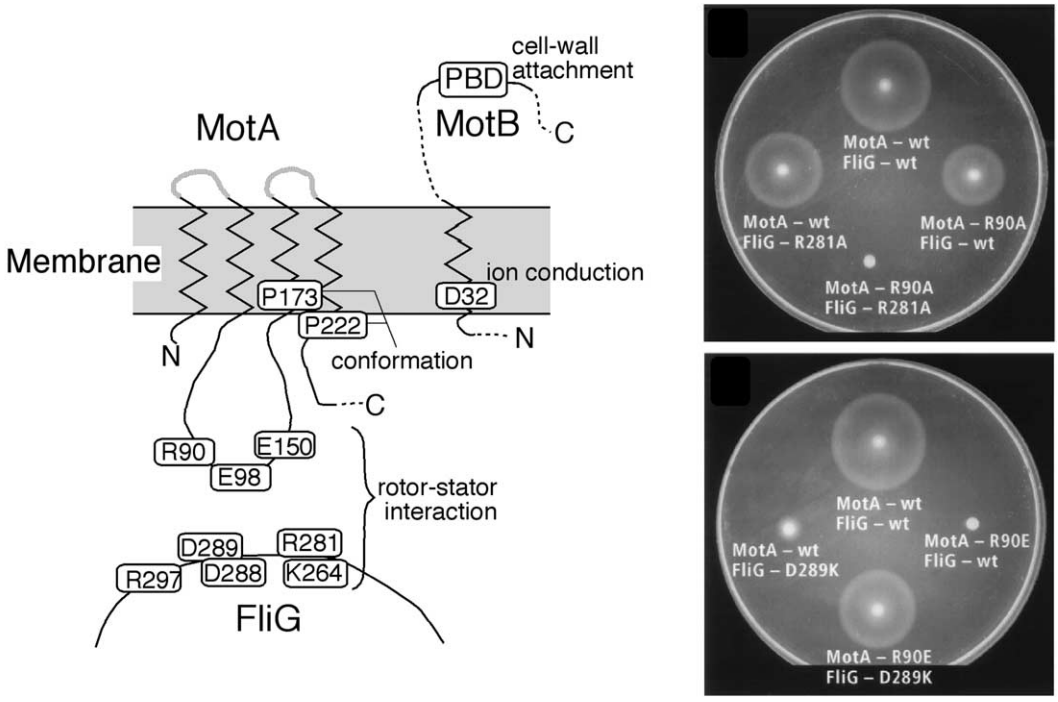

Fig. 4. Left: Functionally important elements of motor proteins, identified in mutational studies. The functional roles of residues are indicated where a probable assignment can be made. The short periplasmic segments of MotA (stippled) do not have conserved critical residues but contain titratable residues that might function collectively to buffer the entrance of the channel. Dashed segments in MotA and MotB are the parts found dispensable for rotation in a study of 10-residue deletions [69]. PBD = peptidoglycan-binding domain. Right: Examples of synergism and suppression seen in FliG–MotA double mutants, demonstrating specific interactions between charged groups on the rotor and stator. Shown are soft-agar plates, on which motile strains move out from the point of inoculation to form circular swarms. Non-motile (or non-chemotactic) strains form smaller, dense colonies. For additional examples of double mutants and a summary of rotor–stator interactions most important for function, see ref. [40].

100% efficiency and a Δp of 160 mV [62], this would imply a stoichiometry of about 70 H^+ per revolution for each torque generator, or $\sim$550 H^+ per revolution for the full motor.

The proton flux through the motor has been measured in experiments using *Streptococcus* cells energized with known, experimentally imposed gradients [66]. Three estimates of stoichiometry were obtained, ranging from 970 to 1450 H^+ per revolution and with an average value of 1140 H^+ per revolution. The measurements were fairly difficult ones and the uncertainties might be great enough to allow a true value around 550. Proton flux has been measured in only one study and additional measurements would be valuable. Whatever the precise proton stoichiometry, the overall rate of proton flow through the motor is notably large, around 200 000 H^+/s for a motor driving a light load at room temperature. The Na^+-driven motor of *Vibrio* must use about a million ions/s, given its greater speed.

Motor rotation presumably occurs by a sequence of discrete events and should thus occur in steps. Steps in the rotation of tethered cells are difficult to see directly, because the flexible hook and filament act as an elastic damper to smooth the motion. By analyzing fluctuations in the rotation speed of tethered cells, Samuel and Berg showed that if the intervals between steps follow a Poisson distribution, then the steps must number about 400 per revolution [67]. If other variable processes also contribute to the speed fluctuations, the number of steps could be larger; if the steps are clocked (i.e. some mechanism exists to decrease the variance in step intervals), then the number of steps could be smaller. A similar analysis was done with motors containing only one or a few torque generators, and showed that the individual torque generators step independently [68].

5. Mutational studies of motor proteins

Mutational studies have identified a number of functionally important features in the proteins that function in rotation (Fig. 4). Most of the MotB protein is in the periplasm [36], and much of this periplasmic domain is dispensable for function [69]. Certain segments in the MotB periplasmic domain are essential for rotation, and probably function to attach the stator to the peptidoglycan [36,70,71]. Some mutations in MotB appear to disrupt function by shifting the stator so that it is misaligned relative to the rotor, and certain of these can be suppressed by mutations in FliG or MotA [72].

Randomly generated mutations in MotA and MotB show a tendency to cluster in the membrane segments, as might be expected for components in an ion-conducting complex [70,73,74]. A conserved Asp residue near the inner end of the MotB membrane segment, Asp 32, is essential for rotation and very likely functions directly in proton transfer [75] (Fig. 4). Tryptophan-scanning mutagenesis of the MotA membrane segments identified helix faces tolerant of bulky replacements, and showed that segments 1 and 2 are more exposed to lipid than segments 3 and 4 [76]. Mutational results were initially interpreted under the assumption that the complex contains a single copy of each protein. The complex is now known to contain multiple copies of MotA and MotB [77–79], and some Trp-scanning results are reinterpreted in that framework below.

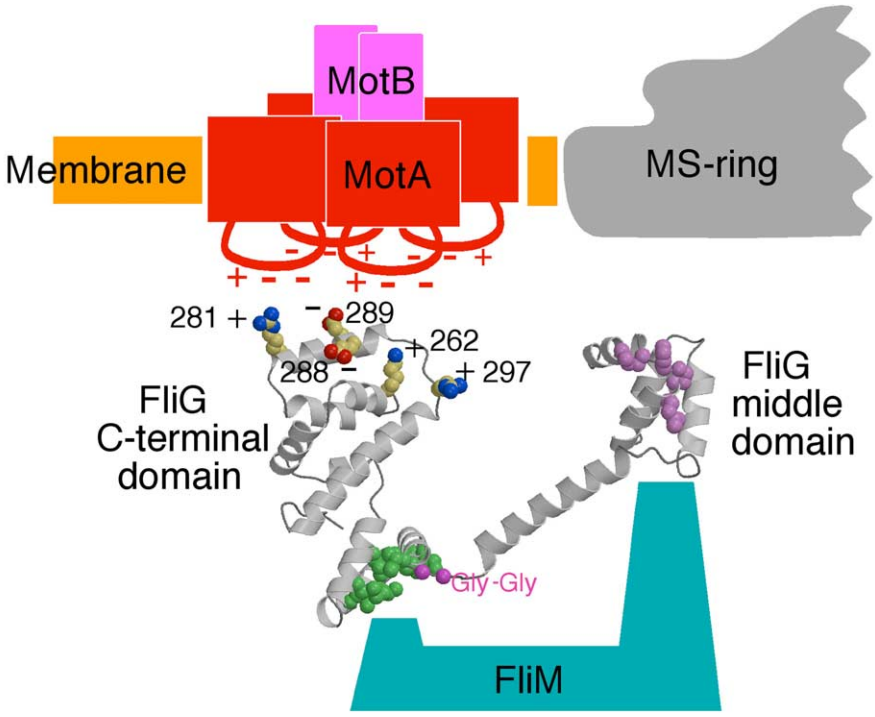

Fig. 5. Structure of FliG-MC (the middle and C-terminal domains of the rotor protein FliG), and hypothesis for the position and orientation of FliG-MC in the flagellar motor. Just one FliG-MC molecule is shown, but a motor actually contains many copies of FliG. The FliG-MC protein consists of two compact, mainly helical domains connected by an α-helix and a linker that includes two consecutive Gly residues. A ridge on the C-terminal domain contains functionally important charged residues that interact with charged residues in the cytoplasmic domain of MotA. The Gly–Gly linker should confer flexibility between the domains. FliM binds to both domains, and so determines the relative orientation of the domains in the flagellum. The flexible linker might function as a hinge to allow movements of the C-terminal domain that occur upon CW–CCW switching. A conserved surface hydrophobic patch is colored green, and a conserved surface-exposed sequence motif (residues EHPQ) is pink; these features might be involved in binding FliM, and/or other proteins in the flagellum. Determinants for binding to the MS-ring are in an N-terminal domain of FliG whose structure is not yet known (adapted from ref. [88]).

Much of MotA is in the cytoplasm, and this part of the protein is also important for rotation as judged by the occurrence of point mutations that disrupt function [80]. The cytoplasmic domain of MotA contains two conserved charge residues (Arg 90 and Glu 98) that are very important for motor rotation in *E. coli*, and a third (Glu 150) that appears to be secondarily important [80]. These residues function collectively, with no single one critical, and charge is their essential property. Two Pro residues near the inner ends of membrane segments 3 and 4 of MotA, Pro 173 and Pro 222, are also conserved and important for rotation [81]. These might regulate the conformation of the MotA/MotB complex, and/or control conformational changes (see below).

Like the cytoplasmic domain of MotA, the C-terminal domain of FliG also contains conserved charged residues that are collectively important for rotation, but not critical individually [82]. Certain combinations of MotA mutations with FliG mutations show strong synergism or suppression, in a pattern that indicates that the charged groups of MotA interact with those of FliG [40] (Fig. 4). Electrostatic interactions between the rotor and stator are thus essential for rotation of the *E. coli* motor. Their precise role in rotation is not known. They might function to couple movements in the stator to rotation of the rotor, or to synchronize events in the stator with the position of the rotor. Since no single charged group at the MotA–FliG interface is critical for rotation, it seems unlikely that these residues form the pathway for protons energizing the motor [40]. The resiliency of this part of MotA, together with the unlikelihood that it functions directly in proton conduction, is further demonstrated by a recent mutational study of PomA, the homolog of MotA found in the Na^+-driven motor of *Vibrio*. Two of the three charged residues implicated in rotation were mutated in this study. The residues previously found to be important in MotA were also the ones most sensitive to mutation in PomA, but for a given mutation the motility defects were less severe in PomA [83]. PomA might contain additional charged residues that contribute to rotor–stator interactions, or the residue not mutated in the PomA study (Asp 128 in PomA, corresponding to Glu 150 in MotA) might play a larger role in *Vibrio* than in *E. coli*.

As noted, FliG does not appear to contain essential binding sites for protons energizing the motor. Mutational studies of FliM and FliN likewise found no protonatable residues (acidic or basic) that are singly critical. Among protonatable residues, only Asp 32 in MotB appears critical. Replacement of Asp 32 with Glu gave poorly functioning motors, and replacement with other residues stopped rotation altogether. Proton conduction can be roughly assayed by a growth impairment that occurs as a result of proton leakage through overexpressed proteins [37]; mutations in Asp 32 blocked proton flow in this assay [75].

If the proton pathway is formed by titratable side-chains of amino acid residues, the mutational results imply that the proton pathway is confined to the stator and includes residue Asp 32 of MotB. This residue is near the inner end of the

MotB membrane segment, close to the cytoplasmic side of the membrane. The Asp residue is conserved in the PomB protein of *Vibrio* [84], and could therefore be the site of ion binding in Na^+-driven motors also. In *Vibrio*, elevated levels of cytoplasmic Na^+ inhibited rotation in the way expected for titration of an interior-facing Na^+-binding site, with apparent dissociation constant ~50 mM [85].

Other binding sites might exist along the proton pathway, but in positions that are not conserved between species. Sequence alignments show that titratable groups are essentially absent from the membrane-embedded segments of MotA and MotB, but are fairly abundant in the short periplasmic segments of MotA and in the segment of MotB just exterior to the membrane. Titratable groups in these segments might buffer the entrance to the channel and facilitate the collection of protons at the rapid rates needed. Mutation of a Glu residue near the entrance to the MotA channel gave a severe motility defect [37,73], and mutation of an Asp residue near the entrance to the PomA channel reduced the motor speed and altered its dependence on Na^+ concentration [86].

6. X-ray structure of a rotor protein

We focused efforts at structure determination on the C-terminal domain of FliG, dubbed FliG-C, because this domain interacts with the stator and functions specifically in rotation. Full-length FliG and FliG-C from *E. coli* failed to crystallize, but FliG-C from the thermophilic bacterium *T. maritima* yielded crystals that diffracted to 2.4-Å resolution [87]. FliG-C is a compact domain formed mainly from α-helices. The functionally important charged residues are found clustered together along a prominent ridge on the protein. On the basis of the mutational studies just described, it was proposed that this ridge is directed toward the stator to allow electrostatic interaction with the charged groups on MotA, and that switching might involve movements of this domain relative to the stator.

The structural study was extended more recently to include the middle domain of FliG, giving further insights into the organization of FliG molecules in the flagellum [88] (Fig. 5). Like the C-terminal domain, the middle domain is formed mainly from α-helices. The middle and C-terminal domains are joined by a Gly-rich linker that should be flexible. FliG binds to FliM, and mutations in FliG that affect this binding [47] cluster in both the middle domain and in the C-terminal domain on a surface opposite the charged ridge. We propose that FliM binds to both the middle and C-terminal domains of FliG, and thereby dictates the relative orientation of these domains in the flagellum. CW–CCW switching might occur by movement of the C-terminal domain of FliG relative to the rest of FliG, under the control of FliM, with the Gly-rich linker serving as a hinge. Manson and co-workers found that replacing one of the linker Gly residues with Ser gave motors that could still rotate in either direction, but reversed less frequently than normal [72].

7. Biochemical studies of the stator complex

There are presently no high-resolution structural data on the MotA/MotB complexes. The topologies of the Mot proteins are known [36,89] (Fig. 4). By a combination of gel-filtration chromatography and quantification of bands on

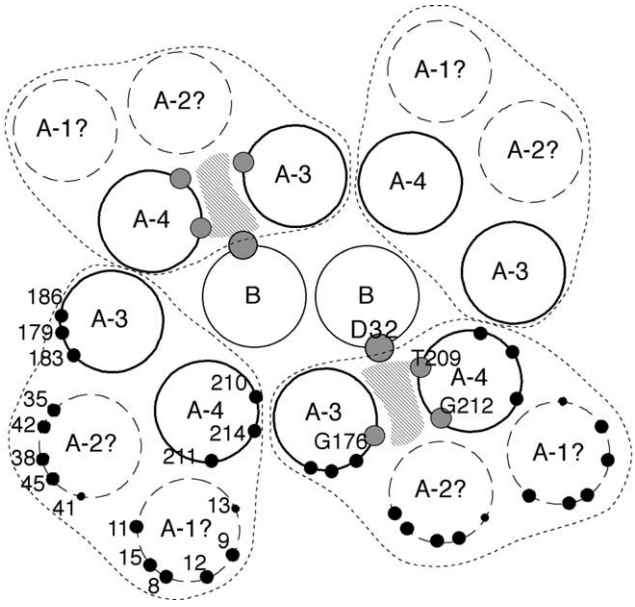

Fig. 6. Hypothesis for the arrangement of membrane segments in the $MotA_4MotB_2$ complex, as deduced from targeted disulfide-crosslinking studies. The view is from the periplasmic side of the membrane. Dashed lines enclose the four segments within each MotA subunit. The arrangement pictured is for the inner (cytoplasmic) halves of the membrane segments, for which crosslinking data are most extensive. The Asp 32 residues of the two MotB molecules (gray circles) are widely separated [79] and most likely function in two distinct proton channels, indicated by crosshatching. Three conserved residues that might face into the channel(s) are indicated (smaller gray circles). MotA segments 1 and 2 appear to be on the outside of the complex, but their precise arrangement has not yet been determined. Black circles indicate positions in the MotA segments where tryptophan replacements were tolerated either fully (large circles) or partially (small circles) [76]. In the MotB segment, Trp was not tolerated at positions in the inner half of the MotB segment (pertinent to the model pictured), but was tolerated at most positions in the outer half (not shown) [100].

Coomassie-stained gels, Sato and Homma obtained evidence that the complex contains four copies of MotA and two copies of MotB [77]. A disulfide-crosslinking study of MotB gave evidence for two MotB molecules in the complex [79], and further crosslinking studies underway (T. Braun, L. al-Mawsawi, and D.F. Blair, in preparation) indicate that the complex contains at least four copies of MotA.

The PomA/PomB complex has been purified and shown to promote transmembrane Na^+ movement when reconstituted into proteoliposomes [77]. The Na^+ flux was less than it must be in the flagellar motor (of the order of 10 ions/s/channel), but nevertheless appears to reflect bona fide channel action, as it was inhibited in the expected ways by a sodium-channel blocker or Li^+. Full channel function might require the additional presence of MotX and MotY, outer-membrane proteins that are also important for rotation of the Na^+ motor in *Vibrio* [90].

Given the stoichiometry $MotA_4MotB_2$ (or $PomA_4PomB_2$), the complex should have a total of 18 membrane segments. Disulfide-crosslinking studies underway are providing an initial picture of their organization (Fig. 6). A dimer of MotB segments is at the center of the complex. Segments 3 and 4 of four MotA molecules are arranged in an inner layer around the MotB segments, and segments 1 and 2 are on the outside, farther from MotB. This arrangement is consistent with Trp-

scanning studies that showed that segments 3 and 4 are likely constrained by other nearby protein segments, whereas segments 1 and 2 are more exposed to lipid [76]. Segments 3 and 4 of MotA, and the MotB segments, appear most important for forming the proton channel(s).

In the structural model arising from the crosslinking experiments, the two MotB segments are oriented so that their critical Asp 32 residues are separated from each where they are likely to function in two distinct channels, rather than a single central channel [79] (Fig. 6). A twin-barrel channel also fits with energy considerations outlined above. Each generator produces a torque that would require about 70 protons per revolution (Section 4 above), whereas the motor contains in the neighborhood of 34 copies of FliG (possibly as few as 26 but probably not more than 50; see Section 3). The measured torque is thus very close to what is expected if two protons pass through a torque generator each time it moves past a FliG subunit. A similar computation of the needed H^+ stoichiometry was made previously by Block and Berg, and they arrived at a similar estimate (65 H^+ per torque generator per revolution; [27]). The kinetic properties of the motor give additional evidence for a twin-barrel torque generator. The torque–speed relation measured by Berry and Berg [58] was accounted for best by assuming that the motor utilizes the energy of two protons simultaneously. It is also worth noting that in simulations of an electrostatic model for the motor, Walz and Caplan [91] could reproduce the measured motor torque only by assuming 22 channels per motor, even more than assumed here.

The structure and mechanism of the stator complexes must be similar in proton-driven and sodium-driven motors, because the rotor of the proton type can be made to work with the stator of the sodium type, and vice versa [92,93]. Chimeric proteins with membrane segments derived from a proton-type stator (Mot proteins from either *E. coli* or *Rhodobacter sphaeroides*) can function with Na^+ ions, which implies that the main determinants of Na^+-specificity are not in the membrane segments [92,94]. The periplasmic domain of PomB is, however, required for Na^+-driven rotation in *Vibrio* cells. This domain might interact with the outer-membrane proteins MotX and MotY, mentioned above. The role(s) of MotX and MotY is not known, but one possibility is that they conduct Na^+ ions across the outer membrane and deliver them to the PomA/B complexes.

The presence of two MotB molecules per stator complex might reconcile an apparent discrepancy between the number of torque generators seen in torque-restoration experiments (eight; [28]) and the number of particles seen in freeze-fracture images (10–12 in *E. coli* and as many as 16 in other species; [25]). If the particles seen in freeze fracture correspond mainly to the periplasmic domain of MotB, then each torque generator could contribute two particles. In *E. coli* membranes the rings do not contain more than 12 particles, whereas 16 might be expected in a motor with a full complement of torque generators. However, the motors in wild-type cells typically do not contain the full complement of generators [28]. Also, if any particles are displaced from the ring during sample preparation they would not be included in the count.

Given the absence of critical titratable groups on the rotor, proton movement must be coupled to rotor movement by some means other than direct binding. An obvious possibility is that proton association/dissociation at Asp 32 drives conformational changes in the stator that apply force to the rotor. To look for conformational changes in the stator, we examined the protease susceptibility of MotA in complex with either wild-type MotB or MotB with various replacements of Asp 32 [95]. The presumption was that the replacement of Asp 32 with asparagine should mimic protonation, by neutralizing the charge and introducing a H-bond donor. Replacement of Asp 32 by asparagine, or by any other small uncharged amino acid, caused a conformational change in MotA that could be detected as a change in protease susceptibility. The sites of altered protease cleavage were in the cytoplasmic domain of MotA, in positions flanking the residues that interact with the rotor. These results support the proposal that protonation of Asp 32 causes a conformational change in the stator, in a part that interacts with the rotor.

8. Hypothesis for the rotation mechanism

Hypotheses for torque generation have been reviewed extensively [15–17,91]) and will not be discussed at length here. In a number of models that have been proposed, protons are assumed to bind to groups on the rotor (e.g. [96]). Such models appear unlikely on grounds given above. In several proposals for the mechanism, protons follow a path within the stator but bind to several sites along the way (e.g. [91,97,98]. These mechanisms also appear unlikely given the finding of only one critical proton-binding group in the stator. In light of the physiological evidence for a powerstroke mechanism [15,58] and biochemical evidence for a conformational change in the stator [95], I suggest that the rotation is driven by cyclic conformational changes in the stator, which occur as protons bind to and dissociate from Asp 32 of MotB. These conformational changes would regulate access to the Asp 32 site to ensure that protons entered the site from the periplasm and departed to the cytosol. The conformational changes in the stator would apply forces to the rotor, most likely on FliG. The effect of the forces – the resultant direction of the push – would be determined by the details of topography at the rotor–stator interface, and switching could occur by changes at this interface. To account for the high duty ratio, the stator would have to remain engaged with the rotor in both (or all) of its conformations. For illustrations of such a mechanism see [81,95]. Among the published proposals for the mechanism it is most similar to an early idea of Lauger (model II in [99]). We can now offer specific suggestions for the proteins and chemical groups involved, reflecting progress in identifying the motor parts.

A better insight into the mechanism will require more structural data on the stator, in both its deprotonated and protonated (or appropriately mutated) states. An atomic picture of the conformational change in the stator should give an immediate insight into the mechanism. Additional structural data on the rotor are also needed, and in order to understand CW–CCW switching structures will be needed for the rotor in both the CW and CCW states. Physiological measurements will continue to play a key role, by providing critical tests of the effects of mutations or other treatments upon motor performance.

Acknowledgements: Work in my laboratory has been supported by grants from the National Science Foundation, the National Institutes of Health, and the University of Utah.

References

[1] Berg, H.C. and Anderson, R.A. (1973) Nature 245, 380–382.
[2] Larsen, S.H., Adler, J., Gargus, J.J. and Hogg, R.W. (1974) Proc. Natl. Acad. Sci. USA 71, 1239–1243.
[3] Shioi, J.-L., Matsuura, S. and Imae, S. (1980) J. Bacteriol. 144, 891–897.
[4] Manson, M.D., Tedesco, P., Berg, H.C., Harold, F.M. and van der Drift, C. (1977) Proc. Natl. Acad. Sci. USA 74, 3060–3064.
[5] Hirota, N. and Imae, Y. (1983) J. Biol. Chem. 258, 10577–10581.
[6] Silverman, M. and Simon, M. (1974) Nature 249, 73–74.
[7] Larsen, S.H., Reader, R.W., Kort, E.N., Tso, W.-W. and Adler, J. (1974) Nature 249, 74–77.
[8] Berg, H. and Brown, D. (1972) Nature 239, 500–504.
[9] Brown, D.A. and Berg, H.C. (1974) Proc. Natl. Acad. Sci. USA 71, 1388–1392.
[10] Aizawa, S.-I. (2001) in: Bacterial Structure, pp. 155–175, Academic Press.
[11] Berg, H.C. (2000) Phil. Trans. R. Soc. Lond. B: Biol. Sci. 355, 491–501.
[12] Macnab, R.M. (2003) Ann. Rev. Microbiol. 57,
[13] Eisenbach, M. and Caplan, S.R. (1998) Curr. Biol. 8, 444–446.
[14] Macnab, R.M. (1995) in: Two-component Signal Transduction (Hoch, J.A. and Silvahy, T.J., Eds.), pp. 181–199, ASM Press, Washington, DC.
[15] Berg, H.C. and Turner, L. (1993) Biophys. J. 65, 2201–2216.
[16] Berry, R.M. and Armitage, J.P. (1999) Adv. Microb. Physiol. 41, 291–337.
[17] Caplan, S.R. and Kara-Ivanov, M. (1993) Int. Rev. Cytol. 147, 97–164.
[18] Samatey, F.A., Imada, K., Nagashima, S., Vonderviszt, F., Kumasaka, T., Yamamoto, M. and Namba, K. (2001) Nature 410, 331–337.
[19] DePamphilis, M.L. and Adler, J. (1971) J. Bacteriol. 105, 384–395.
[20] Khan, I.H., Reese, T.S. and Khan, S. (1992) Proc. Natl. Acad. Sci. USA 89, 5956–5960.
[21] Francis, N.R., Sosinsky, G.E., Thomas, D. and DeRosier, D.J. (1994) J. Mol. Biol. 235, 1261–1270.
[22] Thomas, D., Morgan, D.G. and DeRosier, D.J. (2001) J. Bacteriol. 183, 6404–6412.
[23] Ueno, T., Oosawa, K. and Aizawa, S.-I. (1992) J. Mol. Biol. 227, 672–677.
[24] Thomas, D.R., Morgan, D.G. and DeRosier, D.J. (1999) Proc. Natl. Acad. Sci. USA 96, 10134–10139.
[25] Khan, S., Dapice, M. and Reese, T.S. (1988) J. Mol. Biol. 202, 575–584.
[26] Khan, S., Khan, I.H. and Reese, T.S. (1991) J. Bacteriol. 173, 2888–2896.
[27] Block, S.M. and Berg, H.C. (1984) Nature 309, 470–472.
[28] Blair, D.F. and Berg, H.C. (1988) Science 242, 1678–1681.
[29] Macnab, R.M. (1999) J. Bacteriol. 181, 7149–7153.
[30] Kubori, T., Matsushima, Y., Nakamura, D., Uralil, J., Lara-Tejero, M., Sukhan, A., Galan, J.E. and Aizawa, S.-I. (1998) Science 280, 602–605.
[31] Katayama, E., Shiraishi, T., Oosawa, K., Baba, N. and Aizawa, S.-I. (1996) J. Mol. Biol. 255, 458–475.
[32] Zhao, R., Pathak, N., Jaffe, H., Reese, T.S. and Khan, S. (1996) J. Mol. Biol. 261, 195–208.
[33] Macnab, R. (1992) Annu. Rev. Genet. 26, 129–156.
[34] Dean, G.E., Macnab, R.M., Stader, J., Matsumura, P. and Burke, C. (1984) J. Bacteriol. 143, 991–999.
[35] Stader, J., Matsumura, P., Vacante, D., Dean, G.E. and Macnab, R.M. (1986) J. Bacteriol. 166, 244–252.
[36] Chun, S.Y. and Parkinson, J.S. (1988) Science 239, 276–278.
[37] Blair, D.F. and Berg, H.C. (1990) Cell 60, 439–449.
[38] Stolz, B. and Berg, H.C. (1991) J. Bacteriol. 173, 7033–7037.
[39] Yamaguchi, S., Aizawa, S.-I., Kihara, M., Isomura, M., Jones, C.J. and Macnab, R.M. (1986) J. Bacteriol. 168, 1172–1179.
[40] Zhou, J., Lloyd, S.A. and Blair, D.F. (1998) Proc. Natl. Acad. Sci. USA 95, 6436–6441.
[41] Sockett, H., Yamaguchi, S., Kihara, M., Irikura, V.M. and Macnab, R.M. (1992) J. Bacteriol. 174, 793–806.
[42] Welch, M., Oosawa, K., Aizawa, S.-I. and Eisenbach, M. (1993) Proc. Natl. Acad. Sci. USA 90, 8787–8791.
[43] Irikura, V.M., Kihara, M., Yamaguchi, S., Sockett, H. and Macnab, R.M. (1993) J. Bacteriol. 175, 802–810.
[44] Lloyd, S.A., Tang, H., Wang, X., Billings, S. and Blair, D.F. (1996) J. Bacteriol. 178, 223–231.
[45] Vogler, A.P., Homma, M., Irikura, V.M. and Macnab, R.M. (1991) J. Bacteriol. 173, 3564–3572.
[46] Oosawa, K., Ueno, T. and Aizawa, S.-I. (1994) J. Bacteriol. 176, 3683–3691.
[47] Marykwas, D.L. and Berg, H.C. (1996) J. Bacteriol. 178, 1289–1294.
[48] Tang, H., Braun, T.F. and Blair, D.F. (1996) J. Mol. Biol. 261, 209–221.
[49] Toker, A.S. and Macnab, R.M. (1997) J. Mol. Biol. 273, 623–634.
[50] Francis, N.R., Irikura, V.M., Yamaguchi, S., DeRosier, D.J. and Macnab, R.M. (1992) Proc. Natl. Acad. Sci. USA 89, 6304–6308.
[51] Berg, H.C. (1974) Nature 249, 77–79.
[52] Manson, M.D., Tedesco, P. and Berg, H.C. (1980) J. Mol. Biol. 138, 541–561.
[53] Khan, S. and Berg, H.C. (1983) Cell 32, 913–919.
[54] Khan, S., Dapice, M. and Humayun, I. (1990) Biophys. J. 57, 779–796.
[55] Lowe, G., Meister, M. and Berg, H.C. (1987) Nature 325, 637–640.
[56] Chen, X. and Berg, H.C. (2000) Biophys. J. 78, 1036–1041.
[57] Washizu, M., Kurahashi, Y., Iochi, H., Kurosawa, O., Aizawa, S.-I., Kudo, S., Magariyama, Y. and Hotani, H. (1993) IEEE Trans. Ind. Appl. 29, 286–294.
[58] Berry, R.M. and Berg, H.C. (1999) Biophys. J. 76, 580–587.
[59] Magariyama, Y., Sugiyama, S., Muramoto, K., Maekawa, Y., Kawagishi, I., Imae, Y. and Kudo, S. (1994) Nature 371, 752.
[60] Liu, J.Z., Dapice, M. and Khan, S. (1990) J. Bacteriol. 172, 5236–5244.
[61] Chen, X. and Berg, H.C. (2000) Biophys. J. 78, 2280–2284.
[62] Slonczewski, J., Rosen, B.P., Alger, J.R. and Macnab, R.M. (1981) Proc. Natl. Acad. Sci. USA 78, 6271–6275.
[63] Berry, R.M. and Berg, H.C. (1997) Proc. Natl. Acad. Sci. USA 94, 14433–14437.
[64] Muramoto, K., Sugiyama, S., Cragoe, E.J.J. and Imae, Y. (1994) J. Biol. Chem. 269, 3374–3380.
[65] Ryu, W.S., Berry, R.M. and Berg, H.C. (2000) Nature 403, 444–447.
[66] Meister, M., Lowe, G. and Berg, H.C. (1987) Cell 49, 643–650.
[67] Samuel, A.D. and Berg, H.C. (1995) Proc. Natl. Acad. Sci. USA 92, 3502–3506.
[68] Samuel, A.D.T. and Berg, H.C. (1996) Biophys. J. 71, 918–923.
[69] Muramoto, K. and Macnab, R.M. (1998) Mol. Microbiol. 29 (5), 1191–1202.
[70] Blair, D.F., Kim, D.Y. and Berg, H.C. (1991) J. Bacteriol. 173, 4049–4055.
[71] DeMot, R. and Vanderleyden, J. (1994) Mol. Microbiol. 12, 333–334.
[72] Garza, A.G., Biran, R., Wohlschlegel, J. and Manson, M.D. (1996) J. Mol. Biol. 258, 270–285.
[73] Blair, D.F. and Berg, H.C. (1991) J. Mol. Biol. 221, 1433–1442.
[74] Togashi, F., Yamaguchi, S., Kihara, S.M., Aizawa, S.-I. and Macnab, R.M. (1997) J. Bacteriol. 179, 2994–3003.
[75] Zhou, J., Sharp, L.L., Tang, H.L., Lloyd, S.A., Billings, S., Braun, T.F. and Blair, D.F. (1998) J. Bacteriol. 180, 2729–2735.
[76] Sharp, L.L., Zhou, J. and Blair, D.F. (1995) Proc. Natl. Acad. Sci. USA 92, 7946–7950.
[77] Sato, K. and Homma, M. (2000) J. Biol. Chem. 275, 5718–5722.
[78] Sato, K. and Homma, M. (2000) J. Biol. Chem. 275, 20223–20228.
[79] Braun, T.F. and Blair, D.F. (2001) Biochemistry 40, 13051–13059.
[80] Zhou, J. and Blair, D.F. (1997) J. Mol. Biol. 273, 428–439.
[81] Braun, T.F., Poulson, S., Gully, J.B., Empey, J.C., Van Way, S., Putnam, A. and Blair, D.F. (1999) J. Bacteriol. 181, 3542–3551.
[82] Lloyd, S.A. and Blair, D.F. (1997) J. Mol. Biol. 266, 733–744.
[83] Yorimitsu, T., Sowa, Y., Ishijima, A., Yakushi, T. and Homma, T. (2002) J. Mol. Biol. 320, 403–413.
[84] Asai, Y., Kojima, S., Kato, H., Nishioka, N., Kawagishi, I. and Homma, M. (1997) J. Bacteriol. 179, 5104–5110.

[85] Yoshida, S., Sugiyama, S., Hojo, Y., Tokuda, H. and Imae, Y. (1990) J. Biol. Chem. 265, 20346–20350.
[86] Kojima, S., Shoji, T., Asai, Y., Kawagishi, I. and Homma, M. (2000) J. Bacteriol. 182, 3314–3318.
[87] Lloyd, S.A., Whitby, F.G., Blair, D.F. and Hill, C.P. (1999) Nature 400, 472–475.
[88] Brown, P.N., Hill, C.P. and Blair, D.F. (2002) EMBO J. 21, 3225–3234.
[89] Zhou, J., Fazzio, R.T. and Blair, D.F. (1997) J. Mol. Biol. 251, 237–242.
[90] Okabe, M., Yakushi, T., Kojima, M. and Homma, M. (2002) Mol. Microbiol. 46, 125–134.
[91] Walz, D. and Caplan, S.R. (2000) Biophys. J. 78, 626–651.
[92] Asai, Y., Kawagishi, I., Sockett, R.E. and Homma, M. (1999) J. Bacteriol. 181, 6332–6338.
[93] Gosink, K.K. and Hase, C.C. (2000) J. Bacteriol. 182, 4234–4240.
[94] Asai, Y., Kawagishi, K., Sockett, R.E. and Homma, M. (2000) EMBO J. 19, 3639–3648.
[95] Kojima, S. and Blair, D.F. (2001) Biochemistry 40, 13041–13050.
[96] Meister, M., Caplan, S.R. and Berg, H.C. (1989) Biophys. J. 55, 905–914.
[97] Berry, R.M. (1993) Biophys. J. 64, 961–973.
[98] Elston, T.C. and Oster, G. (1997) Biophys. J. 73, 703–721.
[99] Lauger, P. (1988) Biophys. J. 53, 53–65.
[100] Sharp, L.L., Zhou, J. and Blair, D.F. (1995) Biochemistry 34, 9166–9171.